Adaptive Control Scheme for Clustering of Nodes Based on the Signs of Connections in Dynamical Signed Networks

Qi Wang[1], Yinhe Wang[2], Zilin Gao[3], Peitao Gao[4(✉)], Jianbin Xiong[1], Jian Cen[1,5], and Ying Gao[6]

[1] School of Automation, Guangdong Polytechnic Normal University, Guangzhou 510665, China
[2] School of Automation, Guangdong University of Technology, Guangzhou 510006, China
[3] College of Computer Science and Engineering, Chongqing Three Gorges University, Chongqing 404020, China
[4] School of Electronics and Information, Guangdong Polytechnic Normal University, Guangzhou 510665, China
peitao_gao@sina.com
[5] Guangzhou Intelligent Building Equipment Information Integration and Control Key Laboratory, Guangzhou 510665, China
[6] School of Computer Science and Engineering, South China University of Technology, Guagnzhou 510641, China

Abstract. The concept of clustering has garnered significant attention within the field of complex networks. Numerous clustering algorithms have been documented in the extant academic literature. However, most of them consider static signed networks, which are not suitable for dynamical networks. For dynamical signed networks, there is a class of algorithms called cluster dynamics. Nevertheless, they regard the connection to be time-invariant, which is a constraint. In this paper, for a kind of dynamical signed networks with time-varying connections, we discuss the adaptive control scheme for clustering of nodes, such that the network evolves asymptotically into a classifiable network that contains several friends' groups with clear sign boundaries. In other words, through the careful design of the controller for the nodes and the establishment of coupling relationships between the nodes and their connections, we ensure that the connection of the dynamical signed network can approximate asymptotically the connection of a given classifiable network, as measured by the concept of uniformly ultimately bounded (UUB). Finally, the simulation is used to illustrate the validity of the method proposed in this paper.

This work was supported in part by the Guangzhou Basic and Applied Basic Research Scheme under Grant No. 2023A04J0368, in part by the Introduction of Talents Project of Guangdong Polytechnic Normal University of China under Grant No. 991641250, in part by the National Natural Science Foundation of China under Grant Nos. 62073090, U22A20221, in part by the Natural Science Foundation of Guangdong Province of China under Grant No. 2023A1515011423.

V. C. M. Leung et al. (Eds.): Qshine 2023, LNICST 574, pp. 54–76, 2024.
https://doi.org/10.1007/978-3-031-65123-6_5

Keywords: Multi-clustering · Adaptive control · Classifiable networks

1 Introduction

The field of clustering in complex networks has been very active in the past several years. Clustering is highly valuable in the analysis, design, and optimization of complex systems in real networks and engineering [1]. So far, there have been numerous studies and algorithms developed for detecting communities and clustering in various types of networks [2–7]. However, the application of these methods is not feasible for signed networks. Signed networks are particularly important in social science research as they can represent specific social networks [8–11]. Clustering in signed networks is a noteworthy issue that deserves attention. Therefore, several clustering algorithms have been proposed specifically for signed networks [12–16].

It has been observed that most of the algorithms mentioned above primarily focus on clustering static signed networks. However, there is a need to explore the clustering of dynamical signed networks. In Ref. [17], it was demonstrated that a certain class of dynamical signed networks, which satisfy a specific model, can evolve asymptotically into structural balanced networks. This suggests that the nodes inside these networks can be categorized into one or two friends' groups. Furthermore, Ref. [18] provided the specific rules for changing connections in order to achieve structural balance in the network. However, these studies primarily focused on the behavior of connections and neglected the impact of node states on the connections. In a different study by Ref. [19], it was proven that under certain mathematical conditions, the connection subsystem of a dynamical signed network has the capability to asymptotically achieve a specific structural balance by coupling with the controlled node subsystem. The authors in Ref. [20] introduced a state observer for the connection subsystem and developed a controller utilizing the observer's data. This controller ensures that the states of the connection subsystem asymptotically track structural balance. Additionally, Ref. [21] discussed the tracking problem of the connection subsystem for discrete-time dynamical signed networks. However, these papers grouped the nodes of the signed network only into two friends' groups (two-clustering). How to group the nodes of the dynamical signed network into multiple friends' groups, it should be regarded as the expansion of two-clustering in the above literature.

A class of algorithms based on the phases of the node was proposed in Ref. [9,22]. Here, the phases of two nodes exhibiting positive connections exhibited a progressive convergence, while the phases of two nodes with negative connections had a tendency to diverge from each other. These algorithms can group the nodes into several friends' groups. It is noticed that the results in the above literature [9,22] are suitable only for the nodes with one-dimensional state variables (phase).

In some scenarios, the state of nodes in a network can be multidimensional. This means that a one-dimensional state is not enough to fully describe how the nodes behave dynamically. Therefore, a challenging problem arises: how can we

group nodes with multidimensional states into different friends' groups in signed networks?

The clustering problem for the static signed network is discussed in Ref. [23]. The paper introduces the concept of structural hole and broker, as previously discussed in Ref. [24]. It provides a mathematical proof that a signed network can be classified if and only if it is an unprivileged network. The term "unprivileged network" is defined in Ref. [23] as a network without any brokers. Ref. [25] also discusses the clustering problem, in which the structural hole and broker was not considered. It is noticed that the results in the above literature [23–25] are suitable only to the static signed network, and one can construct an unprivileged network (classifiable network) by using the methods in these papers. However, in the case of a dynamical signed network, it is not natural for the network to evolve into a classifiable state. How can we make a dynamic signed network resemble a given unprivileged network by leveraging the dynamics of its nodes?

In order to sovle the problem described above, we need to consider a dynamical signed network as a large-scale system consisting of two subsystems: the node subsystem and the connection subsystem [26].These subsystems are interconnected, meaning that the dynamics of the node subsystem can influence the dynamics of the connection subsystem through their coupling relationships. This phenomenon is evident in a multitude of real-life instances. For instance, the speeds of motors (nodes) can affect the tension of webs (connections) in multimotor web-winding systems [27,28]; gamma oscillations in neurons (nodes) can lead to synaptic facilitation (connections) in biological neural networks [29]; the alteration in the niche breadth of species (nodes) can have an influence on the level of competition between them (connections) within biological ecosystems [30,31]. The goal is to determine how to make the connection subsystem track a specific unprivileged network, which can be considered as the target for the connection subsystem.

From the above discussion, it is seen that the state dynamics of controlled nodes can be employed to synthesize the coupled relation in the connection subsystem.This interconnected relationship can then influence the connection subsystem to track the given unprivileged network (classifiable network).

Motivated by the preceding discourse, the objective of this scholarly article is to formulate an adaptive control strategy for the nodes and construct the interconnected relationship inside the connection subsystem for a type of dynamical signed networks. By implementing the adaptive controller for the nodes and designing the coupling relationships for the connections, the network will gradually evolve towards a classifiable network (unprivileged network) over time. This means that the network will eventually be grouped into different friends' groups, where the connections within each group are positive, but the connections between different groups are non-positive.

In comparison to previous studies on clustering of nodes, this paper has several notable advantages. Firstly, we consider a class of time-varying dynamical signed networks with the multi-dimensional nodes and synthesis of the coupling relation in connection subsystem. Secondly, a specific unprivileged network

(referred to as a classifiable network) is selected as the target for tracking. This allows for the clustering of nodes within the network into multiple friends' groups (multi-clustering).

The subsequent sections of this paper are structured in the following manner: In section II, we provide the notions of dynamical signed network and classifiable network, and put forth the framework of a dynamical signed network model. What's more, the coupling relationships are given. In section III, an adaptive control scheme for nodes is proposed to make sure the network evolves into a classifiable network overtime via coupling relationships between nodes and connections. In section IV, the simulation example proves the validity of the scheme proposed in this paper. In section V, the conclusion is given.

2 Concept of Classifiable Networks and the Network Model

This paper considers a type of dynamical signed networks. Then, the concept of dynamical signed networks is proposed.

Definition 1 (Dynamical signed network) [23]**.** *If each connection l_{jk} in an undirected -connected signed network can have positive, negative or zero values, this type of network is referred to as a dynamical signed network, with the symbol $\Delta = (U, L)$. The set $U = \{j \,|j = 1, 2, \cdots, N\}$ denotes the sequential labels of its N nodes, and the set $L = \{\, l_{jk}| \, j, k \in U, j \neq k\}$ represents the collection of values corresponding to the real-valued weighted link in the network.*

Based on the definition of a dynamical signed network, it can be inferred that the undirected dynamical signed network $\Delta = (U, L)$ adheres to the condition $l_{jk} = l_{kj}, j, k \in U$, $j \neq k$. Specifically, when j is the same as k, the notation l_{jj} represents the measure of self-join strength for a node. For arbitrary $l_{jk} \in L$, $l_{jk} > 0$, $l_{jk} = 0$, and $l_{jk} < 0$ denote positive connection, non-connection, and negative connection respectively.

Definition 2 (Friends' group) [23]**.** *In the context of a dynamical signed network $\Delta = (U, L)$, a sub-network $\Delta' = (U', L')$ is considered a friends' group if the following conditions hold: for all nodes $j, k \in U'$ and $h \in V - V'$, if the weight l_{jk} between nodes j and k is greater than zero, and the weight l_{jh} between nodes j and h is less than or equal to zero.*

Remark 1. (1) According to Definition 2, it can be observed that the connections inside a given friends' group have a positive nature, whereas the connections between distinct friends' groups are either negative or non-existent. (2) In the case where all connections in the network $\Delta = (U, L)$ are positive, it follows that $U' = U$, $L' = L$, and $l_{jk} > 0$ for every $j, k \in U$. In accordance with Definition 2, every node has the maximum number of friends. Hence, it is its greatest friends' group of itself. (3) In the case where all connections in the network $\Delta = (U, L)$ are non-positive, each node represents a friends' group. In this scenario, the network possesses the highest number of friends' groups. However, each friends' group inside the network is characterized by a minimal amount of elements.

Definition 3 (Classifiable network) [23]. *A dynamical signed network, denoted as* $\Delta = (U, L)$*, is referred to as a p-classifiable network when it consists of p distinct friends' groups. In this context, there exist p friends' groups denoted as* $\Delta_k = (U_k, L_k)$*, where* $k = 1, 2, \cdots, p$*. These friends' groups satisfy the condition that* $U = \bigcup_{k=1}^{p} U_k$*,* $L = \bigcup_{k=1}^{p} L_k \cup (\bigcup_{s,t=1,s\neq t}^{p} L_{st})$*, where* L_{st} *denotes the set containing the connections between two different friends' groups t and s. The network is commonly referred to as a classifiable network, particularly if the variable p is not emphasised.*

Remark 2. In a p-classifiable network, the network $\Delta = (U, L)$ can be categorised into p friends' groups. It can be inferred that the connections among nodes inside a given friends' group are consistently positive, but the connections between two distinct friends' groups are either non-existent or negative.

From the definition of classifiable networks, it is known that not all dynamical signed networks are classifiable. The goal of this paper is to make sure the network evolves into a classifiable network via designing the controller for nodes and the coupling relationships between nodes and connections. To achieve this goal, we first look for a classifiable network, and then let the dynamical signed network tracks this classifiable network over time. As a result, the dynamical signed network can also be classifiable.

The description of the network model is as follow.

We consider an undirected dynamical signed network of N nodes, where both the nodes and connections undergo dynamic changes over time. Assume that each node can be represented by an $n-$dimensional vector, and the dynamical equation governing the behaviour of node i can be mathematically written as:

$$\dot{z}_i = A_i z_i + B_i f_i(z_i), i = 1, 2, \cdots, N \tag{1}$$

where A_i and B_i denote matrices of real numbers with dimensions $n \times n$ and $n \times m$ respectively. $z_i = [z_{i1}, z_{i2}, \cdots, z_{in}]^T$ represents the state variable of node i. $f_i(z_i) = [f_{i1}(z_i), f_{i2}(z_i), \cdots, f_{im}(z_i)]^T \in R^m$. denotes a continuous vector function, where $i = 1, 2, \cdots, N$.

Remark 3. (I) Let A_i be defined as $A_i = \begin{pmatrix} O & I_{n-1} \\ 0 & O^T \end{pmatrix}$ and B_i be defined as $B_i = (O^T \ 1)^T$, where O represents a a zero vector of order $n-1$, I_{n-1} represents a identity matrix with order $n-1$. Eq.(1) may be used to explain several chaotic systems, including Sprott chaotic system[32], Duffing chaotic system[33] and so on. (II) If $B_i = I_m$, where I_m denotes an identity matrix with order m, the Eq. (1) is presented in Ref.[34–36]. (III) If $B_i = \begin{pmatrix} 0 & 1 & 0 \\ 0 & 0 & 1 \end{pmatrix}^T$, then the Lorenz chaotic system, as stated in [37], may be represented by the system (1).

In order to facilitate the subsequent mathematical derivation, we will introduce the notions of matrix vec operator and Kronecker product.

Definition 4 (Matrix Vec Operator) [38]. *Let the matrix $T \in R^{m\times n}$. The $vec(\cdot)$ operator, which maps T onto the vector constructed of the columns of T, can be expressed as follows:*

$$vec(T) = (t_{11}, \cdots, t_{m1}, t_{12}, \cdots, t_{m2}, \cdots, t_{1n}, \cdots, t_{mn})^T \tag{2}$$

Definition 5 (Kronecker product) [38]. *Let the two matrices $S \in R^{p\times q}$ and $T \in R^{m\times n}$, then the Kronecker product of S and T, denoted as $S \otimes T \in R^{pm\times qn}$, is defined as follow:*

$$S \otimes T = \begin{pmatrix} s_{11}T & s_{12}T & \cdots & s_{1q}T \\ s_{21}T & s_{22}T & \cdots & s_{2q}T \\ \vdots & \vdots & \vdots & \vdots \\ s_{p1}T & s_{p2}T & \cdots & s_{pq}T \end{pmatrix} \tag{3}$$

Thus, the aforementioned properties hold true [38]:

(I) $vec(SXT) = (T^T \otimes S)vec(X)$;
(II) $vec(SX+XT) = (I \otimes S + T^T \otimes I)vec(X)$;

Based on system (1), we propose a dynamical equation for nodes with control input u_i that are coupled with connections:

$$\dot{z}_i = A_i z_i + B_i f_i(z_i) + d\sum_{j=1}^{N} l_{ij}(t)G_j(z_j) + u_i \tag{4}$$

where $d > 0$, representing the common connection relationship strength in the network, is a given number. The function $G_j(z_j)$, denoted as $G_j(z_j) = [G_{j1}(z_j), G_{j2}(z_j), \cdots, G_{jn}(z_j)]^T \in R^n$, $j = 1, 2, \cdots, N$ are continuous vector functions. The symbol u_i represents the control input, whereas $l_{ij}(t)$ represents the weight value of the connection between node i and node j at time t.

It is observed that the weight values of the connections between the nodes in Eq.(4) can be represented by the matrix $L = L(t) = (l_{ij}(t))_{N\times N} \in R^{N\times N}$. Let the states vector of nodes $z = [z_1^T, z_2^T, \cdots, z_N^T]^T \in \Gamma \subseteq R^{Nn}$, where Γ is a closed and bounded in R^{Nn}. Let $f(z) = [f_1^T(z_1), f_2^T(z_2), \cdots, f_N^T(z_N)]^T$ and $G(z) = [G_1^T(z_1), G_2^T(z_2), \cdots, G_N^T(z_N)]^T$ be two continuous vector functions. The control vector is denoted as $u = [u_1^T, u_2^T, \cdots, u_N^T]^T$. In conjunction with the matrix Kronecker product formulation, the dynamical Eq. (4) can be reformulated as follows:

$$\dot{z} = Az + Bf(z) + d(L(t) \otimes I_n)G(z) + u \tag{5}$$

where the notion I_n is used to represent an identity matrix of order n. The matrices $A = diag(A_1, A_2, \cdots, A_N)$ and $B = diag(B_1, B_2, \cdots, B_N)$.

In this paper, we consider the time-varying connection relationships, and the connection matrix $L(t)$ satisfies the following Riccati dynamical equation:

$$\dot{L} = \Psi L + L\Psi^T + \Phi(z) \tag{6}$$

where $\Psi \in R^{N\times N}$ is a real number matrix, $\Phi(z) \in R^{N\times N}$ denotes the coupling relationships between the nodes and the connections.

Remark 4. (I) If the weights of the connections are fixed, then $\dot{L} = 0$. Furthermore, when the condition $L_{ii} = -\sum_{j=1,j\neq i}^{N} l_{ij}$ holds, the system (4) is referred to as the time-invariant dissipative coupled complex dynamical network [39–41]. Hence, the constant matrix denoted as L can be considered as a specific instance of the dynamical Eq. (6). On the other hand, in the case when $\dot{L} \neq 0$, it can be inferred that the connections are subject to change over time. Consequently, the system (4) can be seen as a complex dynamical network that exhibits time-varying characteristics, as indicated by previous studies [42,43]. The literature above primarily emphasises the attributes of nodes in Eq. (5), such as synchronisation, whereas the connections serve a secondary function. This research, however, centres its attention on the attributes of connections in Eq. (6), with the nodes assuming a secondary role. (II) It can be seen from the Eq. (5) and Eq. (6) that nodes and connections are coupled via the coupling matrix $\Phi(z)$. That is, the states of connections are affected by the change of the states of nodes via the coupling matrix $\Phi(z)$. Therefore, we can design a controller for nodes to make sure the network evolves into a classifiable network over time. (III) It is important to acknowledge that the network model in Ref. [9,22] was established only by the phases of the nodes. While, in some cases, the state of the nodes is multi-dimensional. Hence, we consider a class of network models with multi-dimensional nodes and synthesis of the coupling relation in connection subsystem.

In this study, the coupling matrix $\Phi(z)$ will be considered as follow:

$$\Phi(z) = -\Psi\left(\hat{L} + \Xi(z)\right) - \left(\hat{L} + \Xi(z)\right)\Psi^T, \xi_{ij}{=}z_i^T z_j \tag{7}$$

where constant matri $\hat{L}$ is unknown, and $\Xi(z) = (\xi_{ij})_{N\times N}$.

Assumption 1. *The vector function $G(z)$ exhibits boundedness. In other words, there exists a positive real number g that is known to meet the inequality $\|G(z)\| \leq g$.*

Assumption 2. *The matrix pair (A, B) exhibits perfect controllability. That is, there exists an $Nm \times Nn$ matrix R for which the Lyapunov equation presented possesses a singular positive definite matrix solution S for any given matrix $Q > 0$:*

$$(A + BR)^T S + S(A + BR) = -Q \tag{8}$$

Remark 5. For the equation shown in Eq. (8), let $W{=}S^{-1}$ and $K = RW$, it is possible to generate matrices S and R by solving linear matrix inequality $WA^T + AW + BK + K^T B^T < 0$. The details illustrated in the Ref. [44].

Assumption 3. *The matrix denoted as Ψ in the context of Eq. (6) exhibits Hurwitz stability.*

Based on Assumption 3, it is evident that the matrix $I \otimes \Psi + \Psi \otimes I$ likewise possesses the property of being Hurwitz. Hence, for any given matrix $\bar{Q} > 0$,

there exists a $N^2 \times N^2$ positive definite matrix J which satisfies the following equation:

$$J\bar{A} + \bar{A}^T J = -\bar{Q} \tag{9}$$

where $\bar{A} = I \otimes \Psi + \Psi \otimes I$.

Assumption 4. *The constant matrix $\hat{L}$, which is unknown, can be denoted as:*

$$\hat{L} = L^* + \mu\Pi \tag{10}$$

where L^* is a predetermined network connection matrix that can be classified. The matrix $\Pi \in R^{N\times N}$ is characterised by having bounded error. There exists an undetermined positive quantity denoted as ε, such that the inequality $\|\Pi\| \leq \varepsilon$ is satisfied. μ is commonly referred to as error coefficient.

Remark 6. In particular, we notice that $\hat{L} = L^*$ for $\mu = 0$ in Eq. (10). In this case, the coupling relationships $\Phi(z)$ in Eq. (7) is directly related to the given tracking target L^*.

Lemma 1. *If Assumption 4 is valid and the coupling relationships $\Phi(z)$ satisfy condition (7), then inequality $\|\Phi(z)\| < \rho$ holds, where ρ is a positive constant number.*

Proof. We can observe from Eq. (9) and Eq. (10):

$$\begin{aligned}
\|\Phi(z)\| &= \left\| -\Psi(\hat{L} + \Xi(z)) - \left(\hat{L} + \Xi(z)\right)\Psi^T \right\| \\
&= \left\| -\Psi(L^* + \mu\Pi + \Xi(z)) - (L^* + \mu\Pi + \Xi(z))\Psi^T \right\| \\
&\leq 2\|\Psi\|\left(\|L^* + \mu\Pi\| + \|\Xi(z)\|\right) \\
&\leq 2\|\Psi\|\left(\|L^*\| + \|\mu\Pi\| + \sqrt{\sum_{i=1}^{N}\sum_{j=1}^{N}\left(z_i^T z_j\right)^2}\right) \\
&\leq 2\|\Psi\|\left(\|L^*\| + |\mu|\varepsilon + \sqrt{\sum_{i=1}^{N}\sum_{j=1}^{N}\left(\|z_i\| \cdot \|z_j\|\right)^2}\right) \\
&= 2\|\Psi\|\left(\|L^*\| + |\mu|\varepsilon + \sqrt{\sum_{i=1}^{N}\|z_i\|^2\sum_{j=1}^{N}\|z_j\|^2}\right) \\
&= 2\|\Psi\|\left(\|L^*\| + |\mu|\varepsilon + \|z\|^2\right)
\end{aligned} \tag{11}$$

Let $\rho = 2\|\Psi\|\left(\|L^*\| + |\mu|\varepsilon + \|z\|^2\right) + \kappa$, where κ is a small positive constant number. We can obtain from Eq.(11):

$$\|\Phi(z)\| < \rho \tag{12}$$

Lemma 1 is proved.

From inequality (12) and Lemma 1, we notice that the states of nodes $\|z\|$ are bounded.

Lemma 2. *If Assumption 3 and Assumption 4 hold, then* $\|L\|$ *is bounded.*

Proof. Considering the characteristics of the Kronecker product, it is possible to express the dynamical Eq. (6) in an alternative form.

$$vec\left(\dot{L}\right) = \bar{A}vec\left(L\right) + vec\left(\Phi(z)\right) \tag{13}$$

Based on Assumption 3, it can be inferred that $\bar{Q} > 0$ and $J > 0$, leading to the following conclusion:

$$\begin{aligned}
&\left[vec(L)^T Jvec\left(L\right)\right]' \\
&= vec\left(\dot{L}\right)^T Jvec\left(L\right) + vec(L)^T Jvec\left(\dot{L}\right) \\
&= \left[\bar{A}vec\left(L\right) + vec\left(\Phi(z)\right)\right]^T Jvec\left(L\right) \\
&+ vec(L)^T J\left[\bar{A}vec\left(L\right) + vec\left(\Phi(z)\right)\right] \\
&= vec(L)^T \bar{A}^T Jvec\left(L\right) + vec(\Phi(z))^T Jvec\left(L\right) \\
&+ vec(L)^T J\bar{A}vec\left(L\right) + vec(L)^T Jvec\left(\Phi(z)\right) \\
&= -vec(L)^T \bar{Q}vec\left(L\right) + 2vec(L)^T Jvec\left(\Phi(z)\right) \\
&- \lambda_{\min}\left(\bar{Q}\right)\left\|vec\left(L\right)\right\|^2 + 2\left\|vec(L)^T\right\|\left\|J\right\|\left\|vec\left(\Phi(z)\right)\right\|
\end{aligned} \tag{14}$$

Let $y = vec(L)^T Jvec\left(L\right)$, we can obtain from (14):

$$y' \leq -\lambda_{\min}\left(\bar{Q}\right)\left\|vec\left(L\right)\right\|^2 + 2\left\|vec(L)^T\right\|\left\|J\right\|\left\|vec\left(\Phi(z)\right)\right\| \tag{15}$$

Divide both sides of inequality (15) by $2\sqrt{y}$ at the same time, we obtain that:

$$\frac{y'}{2\sqrt{y}} \leq -\frac{\lambda_{\min}\left(\bar{Q}\right)\left\|vec\left(L\right)\right\|^2}{2\sqrt{y}} + \frac{\left\|vec(L)^T\right\|\left\|J\right\|\left\|vec\left(\Phi(z)\right)\right\|}{\sqrt{y}} \tag{16}$$

We notice $\lambda_{\min}\left(J\right)\left\|vec\left(L\right)\right\|^2 \leq vec(L)^T Jvec\left(L\right) \leq \lambda_{\max}\left(J\right)\left\|vec\left(L\right)\right\|^2$ holds, then inequality (16) can be reformulated as:

$$\begin{aligned}
(\sqrt{y})' &\leq -\frac{\lambda_{\min}\left(\bar{Q}\right)\left\|vec\left(L\right)\right\|^2}{2y}\sqrt{y} + \frac{\left\|vec(L)^T\right\|\left\|J\right\|\left\|vec\left(\Phi(z)\right)\right\|}{\sqrt{y}} \\
&\leq -\frac{\lambda_{\min}\left(\bar{Q}\right)\left\|vec\left(L\right)\right\|^2}{2\lambda_{\max}\left(J\right)\left\|vec\left(L\right)\right\|^2}\sqrt{y} + \frac{\left\|vec(L)^T\right\|\left\|J\right\|\left\|vec\left(\Phi(z)\right)\right\|}{\sqrt{\lambda_{\min}\left(J\right)}\left\|vec\left(L\right)\right\|} \\
&\leq -\frac{\lambda_{\min}\left(\bar{Q}\right)}{2\lambda_{\max}\left(J\right)}\sqrt{y} + \frac{\left\|J\right\|\left\|vec\left(\Phi(z)\right)\right\|}{\sqrt{\lambda_{\min}\left(J\right)}}
\end{aligned} \tag{17}$$

From Assumption 3, Assumption 4 and Lemma 1, integrating inequality (17), we can obtain:

$$\begin{aligned}
\sqrt{y} &\leq Ce^{\frac{-\lambda_{\min}(\bar{Q})}{2\lambda_{\max}(J)}t} + e^{\frac{-\lambda_{\min}(\bar{Q})}{2\lambda_{\max}(J)}t}\int_0^t \frac{\|J\|\,\|vec\,(\Phi(z))\|}{\sqrt{\lambda_{\min}\,(J)}} e^{\frac{\lambda_{\min}(\bar{Q})}{2\lambda_{\max}(J)}v} dv \\
&\leq Ce^{\frac{-\lambda_{\min}(\bar{Q})}{2\lambda_{\max}(J)}t} + e^{\frac{-\lambda_{\min}(\bar{Q})}{2\lambda_{\max}(J)}t}\int_0^t \frac{2\rho\,\|\Psi\|\,\|J\|}{\sqrt{\lambda_{\min}\,(J)}} e^{\frac{\lambda_{\min}(\bar{Q})}{2\lambda_{\max}(J)}v} dv \\
&\leq Ce^{\frac{-\lambda_{\min}(\bar{Q})}{2\lambda_{\max}(J)}t} + e^{\frac{-\lambda_{\min}(\bar{Q})}{2\lambda_{\max}(J)}t}\int_0^t \frac{2\rho\,\|\Psi\|\,\|J\|}{\sqrt{\lambda_{\min}\,(J)}} e^{\frac{\lambda_{\min}(\bar{Q})}{2\lambda_{\max}(J)}v} dv \\
&= Ce^{\frac{-\lambda_{\min}(\bar{Q})}{2\lambda_{\max}(J)}t} + \frac{4\rho\lambda_{\max}\,(J)\,\|\Psi\|\,\|J\|}{\lambda_{\min}\,(\bar{Q})\,\sqrt{\lambda_{\min}\,(J)}} e^{\frac{-\lambda_{\min}(\bar{Q})}{2\lambda_{\max}(J)}t} \times \left(e^{\frac{\lambda_{\min}(\bar{Q})}{2\lambda_{\max}(J)}t} - 1\right) \\
&= Ce^{\frac{-\lambda_{\min}(\bar{Q})}{2\lambda_{\max}(J)}t} + \frac{4\rho\lambda_{\max}\,(J)\,\|\Psi\|\,\|J\|}{\lambda_{\min}\,(\bar{Q})\,\sqrt{\lambda_{\min}\,(J)}} \times \left(1 - e^{\frac{-\lambda_{\min}(\bar{Q})}{2\lambda_{\max}(J)}t}\right)
\end{aligned} \tag{18}$$

where $C = \sqrt{y\,(0)}, p(t) = e^{\frac{-\lambda_{\min}(\bar{Q})}{2\lambda_{\max}(J)}t}$.

Because $\frac{-\lambda_{\min}(\bar{Q})}{2\lambda_{\max}(J)} < 0$ holds, we obtain $e^{\frac{-\lambda_{\min}(\bar{Q})}{2\lambda_{\max}(J)}t} \to 0, t \to 0$. At the same time, we notice that $y = vec(L)^T Jvec\,(L)$, therefore:

$$\|L\| \leq \sqrt{\frac{y}{\lambda_{\min}\,(J)}} \tag{19}$$

From the result shown in inequality (19), we know that $\|L\|$ is bounded. The proof of Lemma 2 has been completed.

Furthermore, from inequalities (17), (18), and (19), we obtain:

$$\|L\| \to \frac{4\rho\lambda_{\max}\,(J)\,\|\Psi\|\,\|J\|}{\lambda_{\min}\,(\bar{Q})\,\lambda_{\min}\,(J)}, t \to 0 \tag{20}$$

The proof presented above provides evidence for the boundedness of $\|L\|$. Nevertheless, due to the lack of knowledge about the value of ρ in Eq. (20), the upper bound of $\|L\|$ remains uncertain. Let us consider the existence of an unknown positive number H such that the inequality $\|L\| \leq H$ holds. Let $\hat{H}$ denotes the estimation of H, and $\bar{H} = \hat{H} - H$ denotes the estimation error of H.

3 Main Results

Let L^* denotes a given classifiable network connection matrix and $\bar{L} = L - L^*$ denotes the error between connection relationships in the dynamical signed network and a given classifiable network. By utilising Eq. (6) and Eq. (10), we can get the error dynamical equality.

$$
\begin{aligned}
vec(\dot{\bar{L}}) &= vec\left(\dot{L}\right) \\
&= vec\left(\Psi L + L\Psi^T + \Phi\left(z\right)\right) \\
&= vec(\Psi\left(\bar{L}+L^*\right) + \left(\bar{L}+L^*\right)\Psi^T \\
&- \Psi\left(\hat{L} + \Xi\left(z\right)\right) - \left(\hat{L} + \Xi\left(z\right)\right)\Psi^T) \\
&= vec\left(\Psi\bar{L}+\bar{L}\Psi^T\right) + vec\left(\Psi L^*+L^*\Psi^T\right) \\
&- vec\left(\Psi\left(\hat{L} + \Xi\left(z\right)\right) - \left(\hat{L} + \Xi\left(z\right)\right)\Psi^T\right) \\
&= \bar{A}vec\left(\bar{L}\right) + \bar{A}vec\left(L^*\right) - \bar{A}vec\left(\hat{X} + \Xi\left(z\right)\right)
\end{aligned}
\tag{21}
$$

Let us examine the expansion error closed loop system under consideration.

$$
\begin{aligned}
\dot{z} &= Az + Bf(z) + d(L(t) \otimes I_n)G(z) + u \\
vec\left(\dot{\bar{L}}\right) &= \bar{A}vec\left(\bar{L}\right) + \bar{A}vec\left(L^*\right) - \bar{A}vec\left(\hat{L} + \Xi\left(z\right)\right) \\
\dot{\hat{H}} &= \mathrm{T}\left(z, \hat{H}\right) \\
u &= u\left(z, \hat{H}\right)
\end{aligned}
\tag{22}
$$

Control Goal. Consider a dynamical signed network composed of Eq. (5) and Eq.(6). The state vector $Y = \left(z^T, vec\left(\bar{L}\right)^T, \hat{H}\right)^T$ of the expansion error closed-loop system, as depicted in Eq. (22), achieves uniform ultimate boundedness (UUB) by the design of the controller $u\left(z, \hat{H}\right)$ and the adaptive law $\mathrm{T}\left(z, \hat{H}\right)$. In this study, the idea of uniform ultimate boundedness (UUB) is introduced for the state vector $Y = \left(z^T, vec\left(\bar{L}\right)^T, \hat{H}\right)^T$ of the dynamical signed network as mentioned in Ref. [38].

Definition 6 (Uniform Ultimate Boundedness). *The state vector* $Y = \left(z^T, vec\left(\bar{L}\right)^T, \hat{H}\right)^T$ *exhibits uniform ultimate boundedness (abbreviated as UUB) in relation to a closed ball* Ω *if for a given* $t_0 \geq 0$, $d > 0$, *there exists* $T\left(t_0\right)$ *satisfying the following condition:*

$$
\left\|Y\left(t_0\right)\right\| \leq d \Rightarrow \left\|Y\left(t\right)\right\| \in \Omega, t \geq t_0 + T\left(t_0\right) \tag{23}
$$

Remark 7. If the state vector $Y = \left(z^T, vec\left(\bar{L}\right)^T, \hat{H}\right)^T$ in the dynamical signed network is UUB, then the states of the network are bounded for $t \geq t_0 + T\left(t_0\right)$. It means that the error between the connections of the dnetwork and the given classifiable network is bounded. At this moment, the dynamical signed network should also be classifiable. That is, the network's nodes can be categorized into multiple friends' groups.

To attain the aforementioned control goal, the subsequent control scheme is suggested for Eq. (5):

$$u = BRz - Bf(z) + v \tag{24}$$

where $v = -\frac{1}{2}\alpha_1^{-1}S^{-1}z\left\|J\bar{A}\right\|\left(\left\|vec(L^*) + \hat{H}\right\|\right) - \hat{H}d\left\|S\right\|\sqrt{n}gS^{-1}sgn(z)$, and the adaptive law $\dot{\hat{H}}$ satisfies:

$$\dot{\hat{H}} = -\min\left(\frac{\lambda_{\min}(\bar{Q})}{\lambda_{\max}(J)}, \frac{\lambda_{\min}(Q)}{\lambda_{\max}(S)}\right)\hat{H} + \alpha_2\left(\alpha_1^{-1}\left\|J\bar{A}\right\|\|z\|^2 + 2d\|z\|\|S\|\sqrt{n}g\right) \tag{25}$$

Let $sgn(z) = \begin{cases} \frac{z}{\|z\|}, & z \neq 0 \\ 0, & z=0 \end{cases}$ denotes sign function. α_1 and α_2 are two adjustable constants. Matrices S, R and J can be obtained from Eq. (8) and Eq. (9).

Theorem 1. *Let us consider the dynamical signed network consisting of Eq. (5) and Eq. (6). If the* Assumptions *1–4 and the coupling relationships in Eq. (7) are satisfied, then it can be concluded that the state vector denoted as* $Y = \left(z^T, vec(\bar{L})^T, \hat{H}\right)^T$ *of the expansion error closed loop system is UUB when the controller given by Eq.(24) and the adaptive law described in Eq. (25) are employed.*

Proof. Consider the subsequent positive definite function:

$$V = \frac{1}{2}\alpha_1^{-1}vec(\bar{L})^T Jvec(\bar{L}) + z^T Sz + \frac{1}{2}\alpha_2^{-1}\bar{H}^2 \tag{26}$$

Then, the orbit derivative of V can be formulated as:

$$\begin{aligned}
\dot{V} &= \frac{1}{2}\alpha_1^{-1}vec(\dot{\bar{L}})^T Jvec(\bar{L}) + \frac{1}{2}\alpha_1^{-1}vec(\bar{L})^T Jvec(\dot{\bar{L}}) + \dot{z}^T Sz + z^T S\dot{z} + \alpha_2^{-1}\bar{H}\dot{\hat{H}} \\
&= \frac{1}{2}\alpha_1^{-1}\left[\bar{A}vec(\bar{L}) + \bar{A}vec(L^*)\right]^T Jvec(\bar{L}) - \frac{1}{2}\alpha_1^{-1}\left[\bar{A}vec(\hat{L} + \Xi(z))\right]^T Jvec(\bar{L}) \\
&+ \frac{1}{2}\alpha_1^{-1}vec(\bar{L})^T J\left[\bar{A}vec(\bar{L}) + \bar{A}vec(L^*)\right] - \frac{1}{2}\alpha_1^{-1}vec(\bar{L})^T J\left[-\bar{A}vec(\hat{L} + \Xi(z))\right] \\
&+ (Az + Bf(z) + d(L(t) \otimes I_n)G(z) + u)^T Sz + \alpha_2^{-1}\bar{H}\dot{\hat{H}} \\
&+ z^T S(Az + Bf(z) + d(L(t) \otimes I_n)G(z) + u) \\
&= \frac{1}{2}\alpha_1^{-1}vec(\bar{L})^T \bar{A}^T Jvec(\bar{L}) + \frac{1}{2}\alpha_1^{-1}\left[\bar{A}vec(L^*) - \bar{A}vec(\hat{L} + \Xi(z))\right]^T Jvec(\bar{L}) \\
&+ \frac{1}{2}\alpha_1^{-1}vec(\bar{L})^T J\bar{A}vec(\bar{L}) + \frac{1}{2}\alpha_1^{-1}vec(\bar{L})^T J\left[\bar{A}vec(L^*) - \bar{A}vec(\hat{L} + \Xi(z))\right] \\
&+ z^T A^T Sz + z^T SAz + (BRz + d(L(t) \otimes I_n)G(z) + v)^T Sz \\
&+ z^T S(BRz + d(L(t) \otimes I_n)G(z) + v) + \alpha_2^{-1}\bar{H}\dot{\hat{H}}
\end{aligned}$$

$$
\begin{aligned}
&= -\frac{1}{2}\alpha_1^{-1} vec(\bar{L})^T \bar{Q} vec(\bar{L}) + 2z^T S(d(L(t)\otimes I_n)G(z)+v) \\
&+ \alpha_1^{-1} vec(\bar{L})^T J\left[\bar{A} vec(L^*) - \bar{A} vec(\hat{L}+\Xi(z))\right] \\
&+ z^T(A^T S + R^T B^T S + SA + SBR)z + \alpha_2^{-1}\bar{H}\dot{\hat{H}} \\
&= -\frac{1}{2}\alpha_1^{-1} vec(\bar{L})^T \bar{Q} vec(\bar{L}) - z^T Q z + \alpha_1^{-1} vec(L-L^*)^T J\bar{A} vec(L^*) \\
&- \alpha_1^{-1} vec(L-L^*)^T J\bar{A} vec(L^*+\mu\Pi+\Xi(z)) \\
&+ 2z^T S(d(L(t)\otimes I_n)G(z)+v) + \alpha_2^{-1}\bar{H}\dot{\hat{H}} \\
&= -\frac{1}{2}\alpha_1^{-1} vec(\bar{L})^T \bar{Q} vec(\bar{L}) - z^T Q z + \alpha_1^{-1} vec(L)^T J\left[-\bar{A} vec(\mu\Pi) - \bar{A} vec(\Xi(z))\right] \\
&- \alpha_1^{-1} vec(L^*)^T J\left[-\bar{A} vec(\mu\Pi) - \bar{A} vec(\Xi(z))\right] \\
&+ 2dz^T S(L(t)\otimes I_n)G(z) + 2z^T Sv + \alpha_2^{-1}\bar{H}\dot{\hat{H}} \\
&\le -\frac{1}{2}\alpha_1^{-1} vec(\bar{L})^T \bar{Q} vec(\bar{L}) - z^T Q z + \alpha_1^{-1}\left\|vec(L)^T\right\| \left\|J\bar{A}\right\| \|vec(\mu\Pi)\| \\
&+ 2dz^T S(L(t)\otimes I_n)G(z) + \alpha_1^{-1}\left\|vec(L)^T\right\| \left\|J\bar{A}\right\| \|vec(\Xi(z))\| \\
&+ \alpha_1^{-1}\left\|vec(L^*)^T\right\| \left\|J\bar{A}\right\| \|vec(\mu\Pi)\| + \alpha_2^{-1}\bar{H}\dot{\hat{H}} \\
&+ \alpha_1^{-1}\left\|vec(L^*)^T\right\| \left\|J\bar{A}\right\| \|vec(\Xi(z))\| + 2z^T Sv \\
&\le -\frac{\lambda_{\min}(\bar{Q})}{2}\alpha_1^{-1}\left\|vec(\bar{L})\right\|^2 - \lambda_{\min}(Q)\|z\|^2 \\
&+ \alpha_1^{-1}|\mu| H\left\|J\bar{A}\right\| \|vec(\Pi)\| + \alpha_1^{-1} H\left\|J\bar{A}\right\| \|z\|^2 \\
&+ \alpha_1^{-1}|\mu|\left\|vec(L^*)^T\right\| \left\|J\bar{A}\right\| \|vec(\Pi)\| + \alpha_1^{-1}\left\|vec(L^*)^T\right\| \left\|J\bar{A}\right\| \|z\|^2 \\
&+ 2d\left\|z^T\right\| \|S\| H\sqrt{n}g + 2z^T Sv + \alpha_2^{-1}\bar{H}\dot{\hat{H}} \\
&\le -\frac{\lambda_{\min}(\bar{Q})}{2\lambda_{\max}(J)}\alpha_1^{-1} vec\left(\bar{L}\right)^T J vec\left(\bar{L}\right) - \frac{\lambda_{\min}(Q)}{\lambda_{\max}(S)} z^T S z \\
&+ \alpha_1^{-1}(\hat{H}-\bar{H})\left\|J\bar{A}\right\| \|z\|^2 + \alpha_1^{-1}|\mu|\left\|vec(L^*)^T\right\| \left\|J\bar{A}\right\| \varepsilon \\
&+ \alpha_1^{-1}|\mu| H\left\|J\bar{A}\right\| \varepsilon + \alpha_1^{-1}\left\|vec(L^*)^T\right\| \left\|J\bar{A}\right\| \|z\|^2 \\
&+ 2(\hat{H}-\bar{H})d\left\|z^T\right\| \|S\| \sqrt{n}g + 2z^T Sv + \alpha_2^{-1}\bar{H}\dot{\bar{H}} \\
&\le -\min\left(\frac{\lambda_{\min}(\bar{Q})}{\lambda_{\max}(J)}, \frac{\lambda_{\min}(Q)}{\lambda_{\max}(S)}\right)\left[\frac{1}{2}\alpha_1^{-1} vec(\bar{L})^T J vex(\bar{L})\right. \\
&\left. + z^T S z\right] - \min\left(\frac{\lambda_{\min}(\bar{Q})}{\lambda_{\max}(J)}, \frac{\lambda_{\min}(Q)}{\lambda_{\max}(S)}\right)\alpha_2^{-1}\bar{H}\hat{H} \\
&+ \alpha_1^{-1}|\mu|\left\|vec(L^*)^T\right\| \left\|J\bar{A}\right\| \varepsilon + \alpha_1^{-1}|\mu| H\left\|J\bar{A}\right\| \varepsilon \\
&+ \alpha_1^{-1}\left\|vec(L^*)^T\right\| \left\|J\bar{A}\right\| \|z\|^2 + \alpha_1^{-1}\hat{H}\left\|J\bar{A}\right\| \|z\|^2
\end{aligned}
$$

$$
\begin{aligned}
&+ 2\hat{H}d\left\|z^T\right\|\|S\|\sqrt{n}g + 2z^T Sv\} \\
&+ \bar{H}\{\alpha_2^{-1}\dot{\hat{H}} - \alpha_1^{-1}\left\|J\bar{A}\right\|\|z\|^2 - 2d\left\|z^T\right\|\|S\|\sqrt{n}g \\
&+ \alpha_2^{-1}\min(\frac{\lambda_{\min}(\bar{Q})}{\lambda_{\max}(J)}, \frac{\lambda_{\min}(Q)}{\lambda_{\max}(S)})\hat{H}\} \\
&\leq -\min(\frac{\lambda_{\min}(\bar{Q})}{\lambda_{\max}(J)}, \frac{\lambda_{\min}(Q)}{\lambda_{\max}(S)})\{\frac{1}{2}\alpha_1^{-1}vec(\bar{L})^T Jvec(\bar{L}) \\
&+ z^T Sz + \frac{1}{2}\alpha_2^{-1}\bar{H}^2\} + \min(\frac{\lambda_{\min}(\bar{Q})}{\lambda_{\max}(J)}, \frac{\lambda_{\min}(Q)}{\lambda_{\max}(S)})\frac{1}{2}\alpha_2^{-1}H^2 \\
&+ \alpha_1^{-1}H\left|\mu\right|\left\|J\bar{A}\right\|\varepsilon + \alpha_1^{-1}\left|\mu\right|\left\|vec(L^*)^T\right\|\left\|J\bar{A}\right\|\varepsilon \\
&= -\min(\frac{\lambda_{\min}(\bar{Q})}{\lambda_{\max}(J)}, \frac{\lambda_{\min}(Q)}{\lambda_{\max}(S)})V(t) \\
&+ \min(\frac{\lambda_{\min}(\bar{Q})}{\lambda_{\max}(J)}, \frac{\lambda_{\min}(Q)}{\lambda_{\max}(S)})\frac{1}{2}\alpha_2^{-1}H^2 + \alpha_1^{-1}H\left|\mu\right|\left\|J\bar{A}\right\|\varepsilon \\
&+ \alpha_1^{-1}\left|\mu\right|\left\|vec(L^*)^T\right\|\left\|J\bar{A}\right\|\varepsilon
\end{aligned} \tag{27}
$$

And the inequality (27) can be written as:

$$\dot{V}(t) \leq -\zeta V(t) + \omega \tag{28}$$

where $\omega = \frac{1}{2}\zeta\alpha_2^{-1}H^2 + \alpha_1^{-1}H\left|\mu\right|\left\|J\bar{A}\right\|\varepsilon + \alpha_1^{-1}\left|\mu\right|\left\|vec(L^*)^T\right\|\left\|J\bar{A}\right\|\varepsilon$ and $\zeta = \min(\frac{\lambda_{\min}(\bar{Q})}{\lambda_{\max}(J)}, \frac{\lambda_{\min}(Q)}{\lambda_{\max}(S)})$.

The subsequent outcome can be derived using the process of integration applied to Eq. (28).

$$
\begin{aligned}
V(t) &\leq V(0)e^{-\zeta t} + e^{-\zeta t}\int_0^t \omega e^{\zeta\theta}d\theta \\
&= V(0)e^{-\zeta t} - \frac{\omega}{\zeta}e^{-\zeta t} + \frac{\omega}{\zeta} \leq V(0)e^{-\zeta t} + \frac{\omega}{\zeta}
\end{aligned} \tag{29}
$$

Consider a closed ball Ω as follow: $\Omega = \left\{\left(z^T, vec(\bar{L}), \bar{H}\right)\middle| V(t) \leq \tau + \frac{\omega}{\zeta}\right\}$. It's easily seen that for any given positive number $\tau > 0$, if $t \geq -\frac{1}{\zeta}\ln\frac{\tau}{V(0)}$, we can obtain:

$$\left\|vec(\bar{L})\right\| \leq \sqrt{2\alpha_1(\tau + \frac{\omega}{\zeta})/\lambda_{\min}(J)} \tag{30a}$$

$$\|z\| \leq \sqrt{(\tau + \frac{\omega}{\zeta})/\lambda_{\min}(S)} \tag{30b}$$

$$\bar{H}^2 \leq 2\alpha_2(\tau + \frac{\omega}{\zeta}) \tag{30c}$$

Let $Y = \left(z^T, vec(\bar{L})^T, \hat{H}\right)^T$. From the Definition 6 and inequalities (30), it's seen that the state vector Y is UUB. *Theorem* 1 is proved.

Remark 8. It can be seen from (30) that the error of connection relationships (6) is related to α_1, α_2, ω, and ζ. Hence, a more in-depth examination will be provided in the subsequent sections.

(I) For $\left\|vec(\bar{X})\right\|$: Based on Eq. (30a), it can be observed that if the parameter ζ is fixed, the magnitudes of α_1 and ω have an positive relationship with the magnitude of $\left\|vec(\bar{X})\right\|$. However, a decrease in the magnitude of α_1 may lead to an increase in the magnitude of ω and an increase in the gain of the controller in Eq. (24). Conversely, a larger magnitude of α_2 may lead to a greater increase in the adaptive law gain as shown in Eq. (25). Therefore, it is imperative to select the parameters α_1 and α_1 in a comprehensive manner.

(II) For $\|z\|$: Based on Eq. (30a), it can be observed that if the parameter ζ is fixed, an increase in the magnitudes of α_1 and α_2 leads to a decrease in the magnitude of ω. Furthermore, when the magnitude of ω decreases, the magnitude of $\|z\|$ also decreases. Nevertheless, larger magnitudes of α_1 and α_2 may lead to a greater increase in the gain of the adaptive law in Eq. (25). Hence, it is crucial to select the parameters α_1 and α_2 in a comprehensive manner.

(III) For $\bar{H}^2$: Based on Eq. (30c), it can be observed that if the parameter ζ is fixed, a decrease in the magnitudes of α_2 and ω leads to a decrease in the magnitude of $\bar{H}^2$. In addition, a larger magnitude of α_1 may lead to a decrease in the magnitude of ω. Nevertheless, a decrease in the magnitude of α_2 lead to an increase in the magnitude of ω. A larger magnitude of α_1 may lead to a larger magnitude of the vector $\left\|vec(\bar{X})\right\|$. Therefore, it is imperative to select the parameters α_1 and α_2 in a comprehensive manner.

4 Simulation Example

MATLAB is used to provide the simulation in this paper. In this study, we examine an undirected dynamical signed network consisting of 50 nodes, denoted as $N = 50$. Each node in the network is associated with Lü′s chaotic attractor [45]. Therefore, the dynamical equation governing the behaviour of node i can be mathematically represented as:

$$\dot{z}_j = A_j z_j + B_j f_j(z_j) \tag{31}$$

where $z_j = [z_{j1}\ z_{j2}\ z_{j3}]^T$ denotes the states of the node j. Matrix $A_j = \begin{bmatrix} -36 & 36 & 0 \\ 0 & 20 & 0 \\ 0 & 0 & -3 \end{bmatrix}$, matrix $B_j = \begin{bmatrix} 0 & 0 \\ 1 & 0 \\ 0 & 1 \end{bmatrix}$. Vector function $f_j(z_j) = \begin{bmatrix} -z_{j2}z_{j3} \\ z_{j1}z_{j2} \end{bmatrix}$, $j = 1, 2, \cdots, N$.

The dynamical equations of the nodes and the connections are expressed in the forms of (5) and (6). What's more, we choose the coupling relationships shown in (7).

The simulation parameters in this paper are selected in the following manner:

(I) The common connection relationship strength $d = 0.01$, α_1=100, α_2=100.
(II) According to the following steps to generate a classifiable network L^* randomly:

Step 1. Give a groups data $\gamma_i(\gamma_i \in R^{b_i}, i = 1, 2, \cdots, a)$ randomly (the states of the a groups nodes). Choose function $rand$ to generate γ_i, such that the elements of these vectors γ_i^t are within $[1, 2]$, $[3, 4]$, $[5, 6]$ respectively, where $i = 1, 2, \cdots, a$, $t = 1, 2, \cdots, b_i$. Choose $a = 3$, $b_1 = 20$ and b_2=b_3= 15 in this paper.

Step 2. Let l_{mn}^{jk} denotes the connection between the node j in the group m and the node k in the group n, where $m, n = 1, 2, \cdots, a$, $j, k = 1, 2, \cdots, b_i$. Use the following methods to generate a classifiable network connection matrix L^*:

$$l_{mn}^{jk} = \begin{cases} \gamma_m^j \gamma_n^k, m = n, j \neq k \\ round(s) * \left| \gamma_f^j \gamma_h^k \right|, m \neq n \end{cases} \tag{32}$$

where $s = -rand(1)$.

Use $\theta_1 = rand(N, 1)$ to generate a random vector, and let $\Theta_1 = \theta_1 \theta_1^T$, $\Theta_1 \in R^{N \times N}$. Choose $\Theta = 2 * (\Theta_1 - 0.5E)$, where $E = \begin{bmatrix} 1 \\ 1 \\ \vdots \\ 1 \end{bmatrix}_{N \times 1} \times [1\ 1 \cdots 1]_{1 \times N}$.

Therefore, each element in matrix Θ belongs to $[-1, 1]$. Let μ= 0.5. We can get $\hat{L}$ with Eq. (10).

Generate a Hurwitz matrix Ψ with the following steps:

Step 1. Generate n ($n = \frac{N}{2}$) second-order Hurwitz matrices $\Lambda_i = \begin{pmatrix} a_i & b_i \\ c_i & d_i \end{pmatrix}$, $i = 1, 2, \cdots, n$ randomly. That is, $a_i + d_i < 0$ and $a_i d_i - b_i c_i > 0$ hold. Construct an N order block diagonal matrix $\Lambda = diag(\Lambda_1, \Lambda_2, \cdots, \Lambda_n)$.

Step 2. Choose an N order reversible real matrix. Let Ψ=$\lambda * D\Lambda D^{-1}$, where λ=5.

Choose $Q = 0.05 * I_{Nn \times Nn}$, $\bar{Q} = 0.01 * I_{N^2 \times N^2}$. In the simulation, the corresponding parameters can be obtained as follow: we choose the continuous vector function $G_j(z_j) = [5\cos(z_{j1}z_{j2}z_{j3}), 5\cos(z_{j1}z_{j2}z_{j3}), 5\cos(z_{j1}z_{j2}z_{j3})]^T$, $j = 1, 2, \cdots, 50$. Matrices R, S, and J can be obtained from the Lyapunov equations shown in Eq. (8) and Eq. (9). Then we can obtain $g = 61.24$, $\lambda_{\min}(\bar{Q}) = 0.01$, $\lambda_{\min}(Q) = 0.05$, $\lambda_{\max}(J) = 0.46$, $\lambda_{\max}(S) = 0.33$. Choose the initial states of nodes $z(0) = 10 * (rand(1, N) - 0.5E)$ and the initial connections matrix $L(0) = \omega + \omega^T$, where ω= $2 * (rand(N) - 0.5E)$ and $E = \begin{bmatrix} 1 \\ 1 \\ \vdots \\ 1 \end{bmatrix}_{N \times 1} \times [1\ 1 \cdots 1]_{1 \times N}$.

Therefore, it implies that the initial states of nodes and the elements of the initial connections matrix belong to $[-5, 5]$ and $[-2, 2]$ respectively. Choose $\hat{H}(0) = 0.1$.

The simulation results are shown as follows.

From Fig. 1, we notice that associated with the controller for the nodes, the states of the nodes rapidly approach to zero and oscillate within a small amplitude.

In Fig. 2, it's seen that the connections inside the network consisting of (5) and (6) can be categorized into three friends' groups. From the composition rules of the network, we can know that the nodes of the network can also be categorized into three friends' groups. In other words, the network is classifiable at the moment.

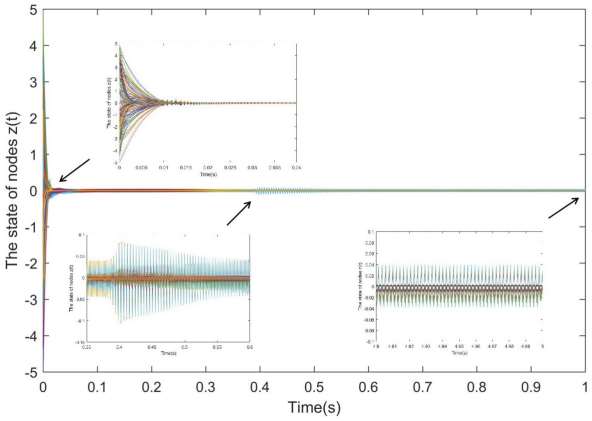

Fig. 1. The state response curves of nodes

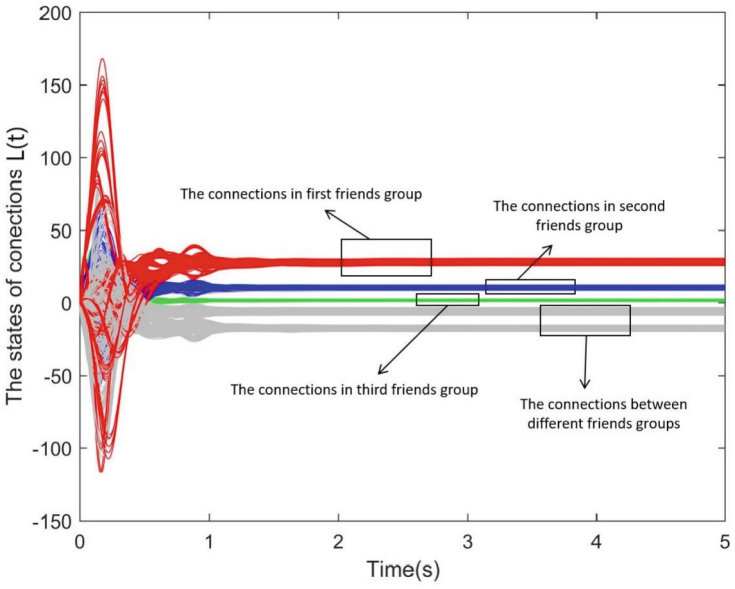

Fig. 2. The state response curves of the connections

In Fig. 3, each curve represents the error between the connection and the target. We notice that the errors approach to zero and are bounded over time after an oscillation. That is, the connections of the network can track the target in the sense of UUB.

From Fig. 4, we notice that the estimate value $\hat{H}$ are monotonically decreasing and bounded.

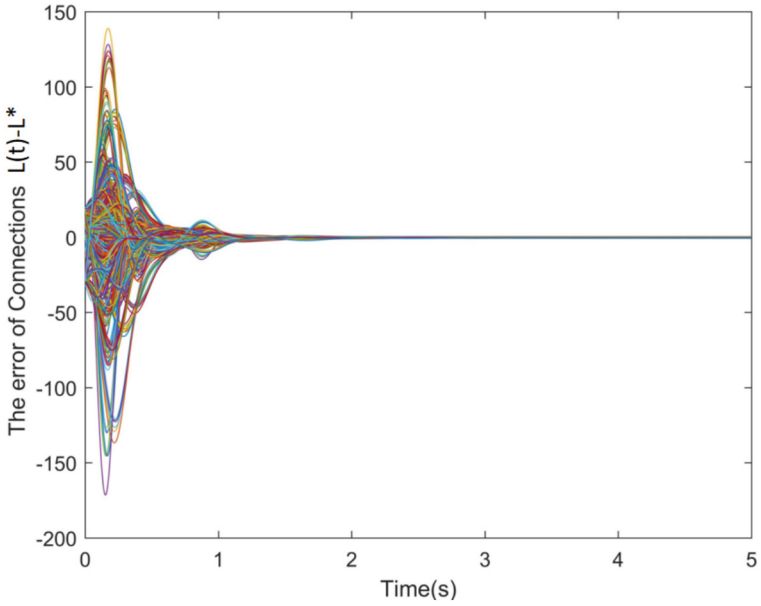

Fig. 3. Response curves of state error $\bar{L}$ of connections

From Fig. 1, Fig. 2, Fig. 3, it can be observed that the dynamical signed network's connections have the ability to track a given classifiable network L^*. This is achieved by the implementation of a controller for nodes and the coupling relationships between nodes and connections. The coupling relationships $\Phi(z)$ are of significant importance in this context.

What's more, from Fig. 1, Fig. 2, Fig. 3, when the states of connections track a given classifiable network, the states of nodes in Fig. 1 oscillate with smaller amplitude, while the states of the connections in Fig. 2 remain stable. It implies that the states of the connections have robustness.

From Fig. 1 and Fig. 3, we notice that when the states of connections track a given classifiable network, the states of nodes in Fig. 1 oscillate with smaller amplitude. In the context of biology, this phenomenon can serve as a rationale for the assertion that "Gamma oscillations can induce synaptic facilitation within biological neural networks."

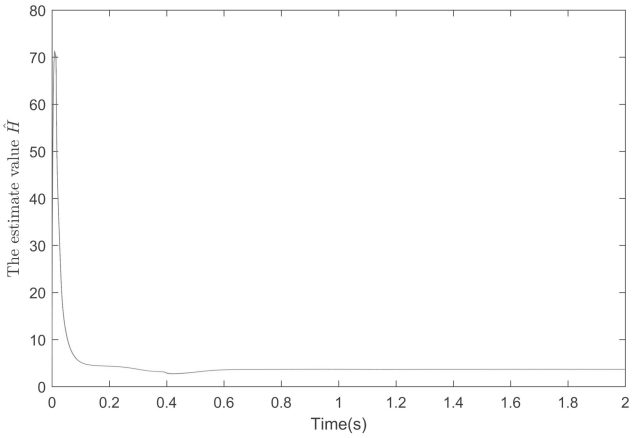

Fig. 4. The time response curve of estimate value $\hat{H}$

In order to observe the results of this experiment more intuitively, we use the method proposed in Ref. [23] to draw the clustering of the nodes when the network reaches stability (track a classifiable network) with the controller. Firstly, we grouped the nodes into m groups according to the connection matrix, so that the connections between the nodes in the same friends' group are positive and the connections between different friends' groups are negative or zero. Assume that m_i denotes the number of nodes in the group i $(i = 1, 2, \cdots, m)$. Use the function $rand$ to assign values for the nodes of group i, denoted as a_f^i, $f = 1, 2, \cdots, m_i$:

$$a_f^i = 10 * (-1)^{randi([1,2]1,1)} rand(1,1) \tag{33}$$

In order to maximize visibility, we employ a strategy of grouping nodes within a specific range based on their affiliation within the same friends' group.

Step 1. Utilise the provided function to compute the coordinates of the x-axis, y-axis, and z-axis for the first node $A_1^i = (x_1^i, y_1^i, z_1^i)$ within each group:

$$\begin{aligned} x_1^i &= \left|a_1^i\right| \\ y_1^i &= 10 * rand(1,1) \\ z_1^i &= x_1^i \end{aligned} \tag{34}$$

Step 2. The coordinates of the remaining groups of nodes are produced in the following manner:

$$\begin{aligned} x_s^i &= \frac{a_s^i}{\max(|a_r^i|)} + \left\lfloor x_1^i \right\rfloor \\ y_s^i &= y_1^i - 2 + 4 * rand(1,1) \\ z_s^i &= x_1^i \end{aligned} \tag{35}$$

where $i = 1, 2, \cdots, m$, $s = 2, 3, \cdots, m_i$ and $r = 1, 2, \cdots, m_i$.

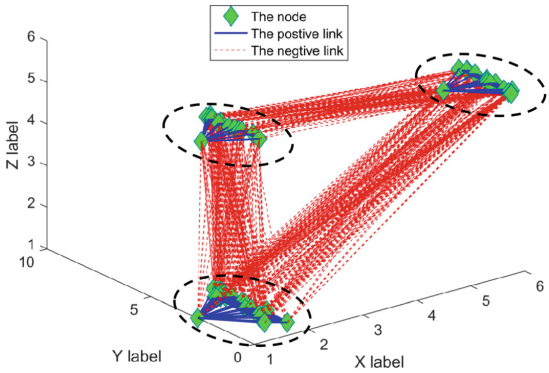

Fig. 5. The clustering of the nodes in dynamical signed networks

The observation of Fig. 5 reveals the presence of three distinct friends' groups, each characterised by a clearly defined boundary. The relationships within the same friends' group exhibit positive connections, while the connections between distinct friends' groups are either negative or non-existent.

5 Conclusion

This research considers the dynamical signed network as a large-scale system consisting of the dynamical node subsystem and the dynamical connection subsystem. The primary focus is on examining the dynamical clustering problem pertaining to the nodes. In contrast to algorithms that treat nodes as one-dimensional state variables, we consider the multi-dimensional nodes coupled with the connections. In this study, we have mathematically formulated a dynamical model for a dynamical signed network. Furthermore, we have rigorously demonstrated that the connections within this network can effectively resemble a predetermined classifiable network in the sense of UUB. This achievement has been accomplished by the design and implementation of a controller specifically tailored for the node subsystem. The network has the capability to dynamically evolve into many friends' groups, which is facilitated by the controller for the node subsystem. If the nodes inside the network can be categorized into one or two distinct friends' groups, then the network exhibits structural balance. Furthermore, it should be noted that the nodes and connections in the network are mutually coupled, meaning that the state dynamics of the node subsystem can have an impact on the dynamics of the connection subsystem through their coupling relationships. Hence, the configuration of the interconnections and the relationships among the nodes are of utmost importance.

References

1. He, C., Liu, H., Tang, Y., et al.: Similarity preserving overlapping community detection in signed networks. Fut. Gener. Comput. Syst. Int. J. Escience **116**, 275–290 (2021)
2. Newman, M., Girvan, M.: Finding and evaluating community structure in networks. Phys. Rev. E **69**(2), 1–15 (2004)
3. Wang, Z., Wang, C., Li, X., et al.: Evolutionary Markov dynamics for network community detection. IEEE Trans. Knowl. Data Eng. **34**(3), 1206–1220 (2022)
4. Hu, L., Pan, X., Tang, Z., et al.: A fast fuzzy clustering algorithm for complex networks via a generalized momentum method. IEEE Trans. Fuzzy Syst. **30**(9), 3473–3485 (2022)
5. Inuwa-Dutse, I., Liptrott, M., Korkontzelos, I.: A multilevel clustering technique for community detection. Neurocomputing **441**, 64–78 (2021)
6. Xu, X., Xiao, Y., Yang, X., et al.: Attributed network community detection based on network embedding and parameter-free clustering. Appl. Intell. **52**(7), 8073–8086 (2022)
7. Qin, H., Li, R., Wang, G., et al.: Mining stable communities in temporal networks by density-based clustering. IEEE Trans. Big Data **8**(3), 671–684 (2022)
8. Yin, X., Hu, X., Chen, Y., et al.: Signed-PageRank: an efficient influence maximization framework for signed social networks. IEEE Trans. Knowl. Data Eng. **33**(5), 2208–2222 (2021)
9. Wu, J., Zhang, L., Li, Y., et al.: Partition signed social networks via clustering dynamics. Physica A-Stat. Mech. Appl. **443**, 568–582 (2016)
10. Hosseini-Pozveh, M., Ghorbanian, M., Tabaiyan, M.: A label propagation-based method for community detection in directed signed social network. Physica A-Stat. Mech. Appl. **604**, 127875 (2022)
11. Li, L., Gu, K., Zeng, A., et al.: Modeling online social signed networks. Physica A-Stat. Mech. Appl. **495**, 345–352 (2018)
12. Sun, R., Chen, C., Wang, X., et al.: Stable community detection in signed social networks. IEEE Trans. Knowl. Data Eng. **34**(10), 5051–5055 (2022)
13. Qi, L., Xu, X., Zhang, X., et al.: Structural balance theory-based e-commerce recommendation over big rating data. IEEE Trans. Big Data **4**(3), 301–312 (2018)
14. Zhong, Z., Wang, X., Qu, C., et al.: Efficient algorithm based on non-backtracking matrix for community detection in signed networks. IEEE Trans. Netw. Sci. Eng. **9**(4), 2200–2211 (2022)
15. Tselykh, A., Vasilev, V., Tselykh, L.: Clustering method based on the elastic energy functional of directed signed weighted graphs. Physica A-Stat. Mech. Appl. **523**, 392–407 (2019)
16. He, C., Fei, X., Cheng, Q., et al.: A survey of community detection in complex networks using nonnegative matrix factorization. IEEE Trans. Comput. Soc. Syst. **9**(2), 440–457 (2022)
17. Marvel, S., Kleinberg, J., Kleinberg, R., et al.: Continuous-time model of structural balance. Proc. Natl. Acad. Sci. USA **108**(5), 1771–1776 (2011)
18. Antal, T., Krapivsky, P., Redner, S.: Social balance on networks: the dynamics of friendship and enmity. Physica D **224**(1), 130–136 (2006)
19. Gao, Z., Wang, Y., Zhang, L., et al.: The dynamic behaviors of nodes driving the structural balance for complex dynamical networks via adaptive decentralized control. Int. J. Mod. Phys. B **32**(24), 1–19 (2018)

20. Gao, Z., Wang, Y., Xiong, J., et al.: Robust state observer design for dynamic connection relationships in complex dynamical networks. Int. J. Control Autom. Syst. **17**(2), 336–344 (2019)
21. Liu, L., Wang, Y., Gao, Z.: Tracking control for the connection relationships of discrete-time complex dynamical network associated with the controlled nodes. Int. J. Control Autom. Syst. **17**(2), 2252–2260 (2019)
22. Chen, J., Wang, H., Wang, L., et al.: A dynamic evolutionary clustering perspective: Community detection in signed networks by reconstructing neighbor sets. Phys. A **447**, 482–492 (2016)
23. Wang, Q., Wang, Y., Gao, Z., et al.: The necessary and sufficient condition for clustering of nodes based on the signs of connections in generalized signed networks. Int. J. Mod. Phys. B **33**(10), 195008610 (2019)
24. Burt, R.S.: Structural Holes: The Social Structure of Competition, pp. 18–23. Harvard University Press, Cambridge (1992)
25. Ma, Y., Zhu, X., Yu, Q.: Clusters detection based leading eigenvector in signed networks. Phys. A **523**, 1263–1275 (2019)
26. Gao, Z., Wang, Y., Ma, J.: The structural balance analysis of complex dynamical networks based on nodes' dynamical couplings. PLoS ONE **13**(1), e01919411 (2018)
27. Chu, X., Nian, X., Sun, M., et al.: Robust observer design for multi-motor web-winding system. J. Frank. Inst.-Eng. Appl. Math. **355**(12), 5217–5239 (2018)
28. Nian, X., Fu, X., Chu, X., et al.: Disturbance observer-based distributed sliding mode control of multimotor web-winding systems. IET Control Theory Appl. **14**(4), 614–625 (2020)
29. Veit, J., Hakim, R., Jadi, M., et al.: Cortical gamma band synchronization through somatostatin interneurons. Nat. Neurosci. **20**(7), 951–959 (2017)
30. Swanson, H., Lysy, M., Power, M., et al.: A new probabilistic method for quantifying n-dimensional ecological niches and niche overlap. Ecology **96**(2), 318–324 (2015)
31. Botts, E., Erasmus, B., Alexander, G., et al.: Small range size and narrow niche breadth predict range contractions in South African frogs. Glob. Ecol. Biogeogr. **22**(5), 567–576 (2013)
32. Sprott, J.: A new class of chaotic circuit. Phys. Lett. A **266**(1), 19–23 (2000)
33. Loria, A., Panteley, E., Nijmeijer, H.: Control of the chaotic Duffing equation with uncertainty in all parameters. IEEE Trans. Circ. Syst. **45**(12), 1252–1255 (1998)
34. Li, Q., Liu, S.: Switching event-triggered network-synchronization for chaotic systems with different dimensions. Neurocomputing **311**, 32–40 (2018)
35. Khan, A., Kumar, S.: Measuring chaos and synchronization of chaotic satellite systems using sliding mode control. Optimal Control Appl. Methods **39**(5), 1597–1609 (2018)
36. Mobayen, S., Ma, J.: Robust finite-time composite nonlinear feedback control for synchronization of uncertain chaotic systems with nonlinearity and time-delay. Chaos Solitons Fractals **114**, 46–54 (2018)
37. Peng, C., Li, Y.: Parameters identification of nonlinear Lorenz chaotic system for high-precision model reference synchronization. Nonlinear Dyn. **108**(2), 1733–1754 (2022)
38. Charles, F.: The ubiquitous Kronecker product. J. Comput. Appl. Math. **123**(1–2), 85–100 (2000)
39. Ding, S., Wang, Z.: Synchronization of coupled neural networks via an event-dependent intermittent pinning control. IEEE Trans. Syst. Man Cybern.-Syst. **52**(3), 1928–1934 (2022)

40. Song, X., Man, T., Ahn, C., et al.: Finite-time dissipative synchronization for markovian jump generalized inertial neural networks with reaction-diffusion terms. IEEE Trans. Syst. Man Cybern.-Syst. **51**(6), 3650–3661 (2021)
41. Palanisamy, S., Rathinasamy, S., Choon, K., et al.: Observer-based synchronization of complex dynamical networks under actuator saturation and probabilistic faults. IEEE Trans. Syst. Man Cybern.-Syst. **49**(7), 1516–1526 (2019)
42. Lin, H., Wang, J.: Pinning control of complex networks with time-varying inner and outer coupling. Math. Biosci. Eng. **18**(4), 3435–3447 (2021)
43. Yang, Y., Long, Y.: Event-triggered sampled-data synchronization of complex networks with time-varying coupling delays. Adv. Difference Equ. **2020**(1), 312 (2020)
44. Wang, Y., Fan, Y., Wang, Q., et al.: Adaptive fuzzy synchronization for a class of chaotic systems with unknown nonlinearities and disturbances. Nonlinear Dyn. **69**(3), 1167–1176 (2012)
45. Lu, J., Chen, G., Cheng, D., et al.: Bridge the gap between the Lorenz system and the Chen system. Int. J. Bifurcation Chaos **12**(12), 2917–2926 (2002)